

Application of the Scaling Law for Swept Shock/Boundary-Layer Interactions

Yeol Lee*

Associate Professor, School of Aerospace & Mechanical Engineering, Hankuk Aviation University, Kyunggi-Do 412-791, Korea

An experimental study providing additional knowledge of quasi-conical symmetry in swept shock wave/turbulent boundary-layer interactions is described. When a turbulent boundary layer on the flat plate is subjected to interact with a swept planar shock wave, the interaction flowfield far from fin leading edge has a nature of conical symmetry, which topological features of the interaction flow appear to emanate from a virtual conical origin. Surface streakline patterns obtained from the kerosene-lampblack tracings have been utilized to obtain representative surface features of the flow, including the location of the virtual conical origin. The scaling law for the sharp-fin interactions suggested by previous investigators has been reexamined for different freestream Mach numbers. It is noticed that the scaling law reasonably agrees with the present experimental data, however, that the law is not appropriate to estimate the location of the virtual conical origin. Further knowledge of the correlation for the virtual conical origin has thus been proposed.

Key Words : Shock Wave, Boundary-Layer Interactions, Conical Symmetry, Separation

Nomenclature

L_i	: Inception length
L_s	: Length along inviscid shock line on test surface from fin leading edge
L_{un}	: Normal distance from inviscid shock line on test surface to upstream influence
M_∞	: Freestream Mach number
M_n	: The component of freestream Mach number normal to inviscid shock wave (= $M_\infty \sin \beta_o$)
Re_δ	: Reynolds number based on the incoming boundary layer thickness
X	: Axial directional coordinate from fin leading edge
Z	: Spanwise directional coordinate from fin leading edge

Greek symbols

α	: Angle-of-attack of the fin
β_u	: Azimuth angle of upstream influence line with respect to incoming freestream direction
β_o	: Azimuth angle of inviscid shock with respect to incoming freestream direction
β_s	: Azimuth angle of primary separation with respect to incoming freestream direction
ΔVCO	: Distance between fin leading-edge and virtual conical origin
δ	: Incoming boundary layer thickness at fin leading edge

1. Introduction

The study of shock wave/turbulent boundary-layer interactions has been important and even critical for the design of high-speed vehicles and for the validation of the associated numerical simulations. A strong three-dimensional separated region can be generated in the interaction

* E-mail : ylee@mail.hankong.ac.kr
 TEL : +82-2-300-0113; FAX : +82-2-3158-3189
 Associate Professor, School of Aerospace & Mechanical Engineering, Hankuk Aviation University, Kyunggi-Do 412-791, Korea. (Manuscript Received June 17, 2003; Revised September 9, 2003)

flowfield, especially for strong shocks. Substantial variations in surface pressure, skin friction and heat transfer have been observed to occur in the separated flow region (Kim et al., 1991; Lee et al., 1994), and the variation of those values are of practical importance in establishing the limits of aerodynamic and aerothermal loads on high-speed flight vehicles. A detailed survey of the past work on such interactions was carried out by Settles and Dolling (1986). With detailed flowfield surveys of the sharp fin interactions, important information has become available. This is especially so with regard to a significance of the choice of a coordinate system in the fin interactions.

The most noticeable feature in the interaction is their quasi-conical nature. The quasi-conical symmetry has its practical importance, since the use of such simple assumptions can lead to simple coordinate approach in related studies, and thus can greatly reduce experimental and computational requirements. This feature has been analytically observed by Inger (1987), using an order-of-magnitude analysis of the governing equations, and by many experimental parametric studies (Settles and Lu, 1985; Alvi and Settles, 1991). From those previous studies, it has been noticed that, although the boundary-layer growth cannot be conical, the nature of flowfield in sharp-fin interactions and the interaction growth are approximately conical except for an initial region in the vicinity of the juncture of fin leading edge and model surface. Beyond the initial region, which is called the inception zone, topological features of the interaction flow appear to emanate from a single point, which is termed the 'virtual conical origin (VCO).' A detailed description on the characteristics of the quasi-conical symmetry of sharp-fin interactions is provided in the next section.

Since many previous studies on sharp-fin interactions have been possibly performed in the inception zone, there have been possibilities of misinterpretation of such data. Clear information of the size of the inception zone is thus essential for the proper understanding of any data of the fin interactions. Settles and Lu once proposed a

scaling law to estimate the size of the inception zone (i.e., the inception length) of sharp fin interactions of the freestream Mach number of 3.0 (Settles and Lu, 1985). However, applicability of the scaling law to estimate the inception length for other freestream Mach numbers has not been tested. Knowledge of the VCO is important as well as the inception length, since the VCO is a fundamental base of the theory of the conical symmetry of sharp-fin interactions. However, not much information on it has been available, except the fact that the location of VCO is a highly viscous phenomenon.

The purpose of the present study is, therefore, to provide further information of the quasi-conical nature of the fin interactions. The scaling law previously suggested by Settles and Lu has been reexamined for different freestream Mach numbers, and applicability of the scaling law to estimate the location of the VCO has been considered. Further additional knowledge of the correlation for the location of the VCO is proposed.

2. Quasi-Conical Symmetry

A schematic diagram of the sharp fin-interaction is shown in Fig. 1. In the figure, a two-dimensional turbulent boundary layer on a near-adiabatic flat plate is subjected to interact with a swept planar shock wave generated by a sharp fin at an angle of attack, α . The interaction is "dimensionless," for which the sharp fin imposes no length dimension on the interaction (Settles

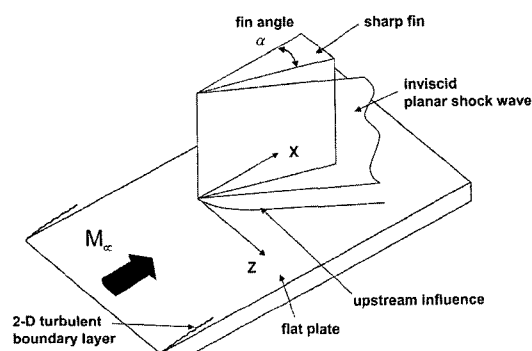


Fig. 1 Sketch of the sharp fin-interaction and test geometry

and Dolling, 1986). The dimensionless fin-generated swept interaction have been shown to display the nature of quasi-conical symmetry about a virtual conical origin, which is located slightly upstream of the fin leading edge. Since the conical symmetry has been originally defined for inviscid flows, the term of "quasi-conical symmetry" is used in the present study.

Figure 2 shows a sketch of the limiting streamlines underneath the sharp fin interaction. The limiting streamlines depicted in the figure include the upstream influence, which is defined where the incoming freestream parallel streamlines are first deflected from their original trajectories, primary separation, and the inviscid shock wave line on test surface. The curved, non-conical region is called the "inception zone," and beyond the region, the topological features of the interaction surface flow appear to emanate from a virtual conical origin (VCO). The inception length, L_i , represents the length along the inviscid shock trace on test surface in the inception zone.

Not only the surface features, but also the flow-field structure above the surface of the interaction shows a quasi-conical behavior (Zubin and Ostapenko, 1979; Alvi and Settles, 1991). Zubin and Ostapenko have provided one of the first discussions of the conical characteristics of sharp-

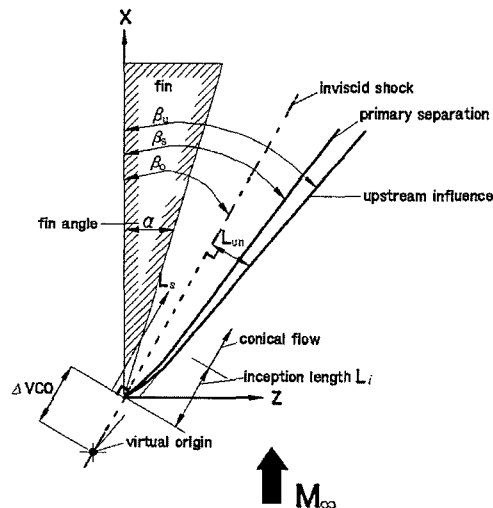


Fig. 2 Limiting streamlines in the sharp-fin interaction

fin interactions. They have proposed that the plateau pressure ratio in the interaction can be correlated as a function of the normal Mach number to the separation line, not the freestream Mach number. By utilizing the conical shadowgraphy, Alvi and Settles have found that the λ -shock structure of the interaction can be aligned accurately with a conical light beam, indicating the nature of conical flowfield (Alvi and Settles, 1991). They have further noticed that the λ -shock bifurcation depends solely on the normal Mach number and is independent of both freestream Mach number and fin angle, which is one of the representative characteristics of the conical symmetry of the flow.

Most noticeable advance in the knowledge of the quasi-conical symmetry of the interaction has been achieved by Dolling and Bogdonoff (1983), and Settles and Lu (1985). Settles and Lu have performed parametric studies on the similarity in three-dimensional fin interactions, and have found that the upstream influence in a sharp-fin interaction of $M_\infty=3.0$ obeys a scaling law associated with the Mach number and the Reynolds number based on the incoming boundary layer thickness, Re_δ . Among other surface flow features in the interaction, the upstream influence is considered as an important parameter, since the onset of separation of incoming boundary layer just after the upstream influence considerably changes overall flow structure of the interaction.

In coordinates normal and tangential to the inviscid shock wave, their scaling law is written for the upstream influence as;

$$(L_{un}/\delta)(Re_\delta^a/M_n) = f[(L_s/\delta)Re_\delta^a] \quad (1)$$

Here, M_n is the normal Mach number, which is the component of the freestream Mach number normal to the inviscid shock wave ($=M_\infty \sin \beta_0$), and L_{un} is the normal distance from inviscid shock line to upstream influence (see Fig. 2). δ is the incoming boundary layer thickness at the fin leading edge. According to Settles and Lu, the constant a in Eq. (1) has an empirical value of about $1/3$ for $M_\infty=3.0$.

From the observation that the simple normalization of L_{un} by M_n effectively correlates

variations in shock strength, Settles and Lu have further revealed that the size of the nonconical inception zone, i.e., the inception length L_i , can be estimated by the scaling law. To demonstrate the theory, they plotted the experimental data of upstream influence, which were obtained by the surface flow visualization for both swept and unswept fin interactions, in the above coordinates shown in Eq. (1). Detailed result of the scaling of upstream influence for a wide range of strengths of fin-angles-of-attack α for $M_\infty=3.0$ can be found in Fig. 9 in their article (Settles and Lu, 1985). From the result, they have further noted that the inception length can be given approximately by ;

$$(L_i/\delta) (\text{Re}_\delta^{1/3}) \approx 1600 \quad (2)$$

However, all their experimental data have been obtained for a single freestream Mach number of 3.0. The applicability of the scaling law to estimate the inception length as shown in Eq. (2) for other freestream Mach number flows have not yet been tested.

3. Experimental Methods

3.1 Test conditions

The supersonic wind tunnel used in the present experiments is intermittent, and blowdown type. The stagnation pressure in the settling chamber is regulated from 0.34 Mpa to 1.65 Mpa, and once the stagnation pressure is set for a given test condition, it is kept almost constant (less than 3 % variation) during the tunnel run. The stagnation temperature of the freestream is approximately near to the ambient temperature. The size of the test section is 150 mm in width, 170 mm in height, and 600 mm in length. The tunnel can control the freestream Mach numbers from 1.5 to 4.0 in the test section.

A flat plate is installed inside the test section to generate an undisturbed two-dimensional turbulent boundary layer. Natural boundary-layer transition on the plate typically occurs within 1~2 cm of the plate leading edge at the present high Reynolds number flows. The turbulent boundary layer on the plate is in a near-adiabatic condition

Table 1 Typical freestream test conditions and the incoming boundary layers

freestream Mach number		3.0	4.0
total pressure (kpa)		850	1,480
total temperature (K)		275	288
unit Reynolds number (1/m)		6.8×10^7	7.0×10^7
incoming boundary layer (mm)	δ	3.6	3.1
	δ^*	1.1	1.0
	θ	0.2	0.1

(the ratio of the wall temperature, T_w , to the adiabatic wall temperature, T_{aw} , is typically 1.03, and the recovery factor is approximately 0.9). The tabulated data on the typical freestream test conditions (without fin installation) are listed in Table 1. Integral properties of the incoming boundary layer in Table 1 have been measured at 227 mm downstream of the plate leading edge.

The fin leading edge is located 216 mm downstream of plate leading edge. The size of the fin is small enough to avoid blockage of the flow in the test section, but large enough to generate a "dimensionless" interaction on the flat plate. The strength of the planar shock generated by the fin is controlled by changing the angle of attack of the fin, which is manipulated by a pneumatic fin-injection mechanism.

3.2 Measurement technique

Various diagnostic techniques, including surface pressure measurements, surface flow visualization, measurements of skin friction and heat transfer, have been employed for the study of shock/boundary-layer interactions. Only experimental results from the surface flow visualization are discussed herein. For the surface flow visualization, the kerosene-lampblack tracing technique has been utilized. When a mixture of kerosene and carbon powder (lampblack) painted on the area of interest of the plate surface is exposed to flow, the mixture is driven to form local streak patterns. During a tunnel run (typically 15 to 20 seconds) the volatile kerosene is evaporated, and only the lampblack remains on the test surface. It is observed that unsteady motions of shock and associated interaction flowfield in high frequency

ranges are not registered by the thin layer of the mixture during the tunnel run. After tunnel is shut down, a 150 mm wide strip of transparent adhesive tape (Scotch Magic Transparent Tape, 3M) is carefully pressed down upon the test surface and rubbed using a soft cloth. Then, the thin coating of carbon pigment remaining on the test surface is transferred to the tape and the tape is pressed onto a sheet of white paper, preserving the "1 : 1 scale" surface streakline pattern. This method yields immediate results without photographic processing and provides full-scale quantitative data, such as measurements of streakline distances and angles. To apply this technique successfully, the ratio of the mixture of components is important. A 4 : 1 mixture of kerosene and carbon powder by volume produces a very thin layer of the mixture over a model surface and prevents the objectionable characteristics of the more common oil-flow techniques (Settles, 1975).

4. Results and Discussion

4.1 Surface flow visualization

In Fig. 3, one example of kerosene-lampblack trace patterns is shown for the freestream Mach number of 4.0 and the fin-angle-of-attack $\alpha=16^\circ$, which is a relatively strong interaction case. The key features such as upstream influence, primary separation, secondary separation, and fin edge are observed in the trace pattern. The parallel streamwise streak pattern upstream of the fin leading edge shows the uniform incoming two-dimensional boundary layer. This incoming flow begins

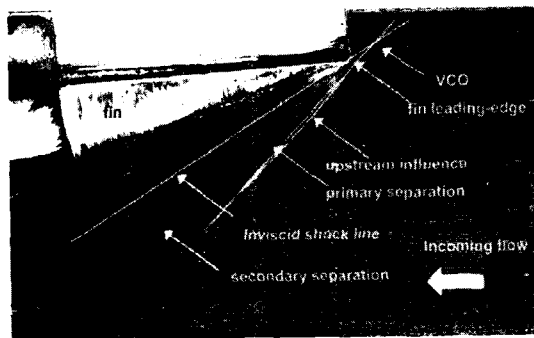


Fig. 3 Surface streakline pattern for $M_\infty=4.0$, $\alpha=16^\circ$

to deflect as it approaches to the fin, and the first turning of the streak patterns depicts the upstream influence, which appears white in the figure.

Immediately thereafter, the incoming boundary layer separates, and a line of pigment (beginning of dark region) represents the primary separation. Such a close distance between the primary separation and upstream influence is a typical phenomenon for the present strong interaction. The secondary separation inside vortex region under the λ -shock structure is also seen in the figure. The VCO is also depicted slightly upstream of the fin leading edge in the figure, determined by intersecting the upstream influence line and the inviscid shock line on test surface.

4.2 Scaling law of upstream influence for $M_\infty=3.5$ and 4.0

Figure 4 shows the result of scaling of upstream influence obtained from the kerosene-lampblack tracings for the freestream Mach numbers of 3.5 and 4.0. Experimental data of the variation of skin friction for the identical interactions are available in the reference (Kim et al., 1991). Since the boundary between the inception and the quasi-conical zones is difficult to determine accurately due to the asymptotic joining of the inception and conical zones, the error band of the boundary is depicted in Fig. 4. The inception length determined from Fig. 4 is approximately ;

$$1400 \leq (L_i/\delta) (Re_\delta^{1/3}) \leq 1700 \quad (3)$$

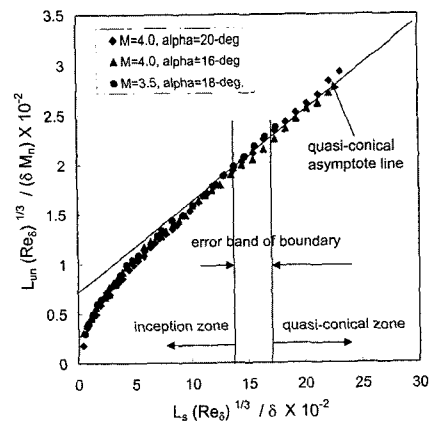


Fig. 4 Scaling of upstream influence in nondimensional form for $M_\infty=3.5$ and 4.0

The range of the inception zone for the present case of $M_\infty=3.5$ and 4.0 is slightly lower than the previous result obtained by Settles and Lu for $M_\infty=3.0$ (see Eq. (2)). The intercept of the asymptote at the coordinate of $L_{un}(Re_\delta)^{1/3}/\delta M_n$ is also slightly less than the value of the previous result. However, the results shown in Fig. 4 shows a reasonable agreement with the previous results by Settles and Lu (1985), if the difficulty associated in estimation of the inception length, L_i , (due to the asymptotic joining of the inception and conical zones) is taken into account. It implies that the scaling law of the upstream influence can be reasonably applied for other freestream Mach numbers in fin-interactions as well as for $M_\infty=3.0$.

Neumann and Hayes have once showed that the peak pressure ratio (a ratio of the peak pressure inside interaction to the pressure of the freestream) could be correlated with the normal Mach number (Neumann and Hayes, 1977). For wide range of freestream Mach numbers from 2.95 to 5.85, they have found that the peak pressure ratio could be correlated as M_n^{np} , and that the exponent, np , depended on the measurement locations X/δ , where X is the streamwise distance from fin leading edge. Figure 5 shows their fairing of data for the correlation and the dependency of np with X/δ . In the figure, the np increases asymptotically as X/δ increases, and it approaches a fixed value of 2.4 for X/δ larger than approximately 30. It implies that the boundary between the inception and conical zones occurs near $X/\delta=30$

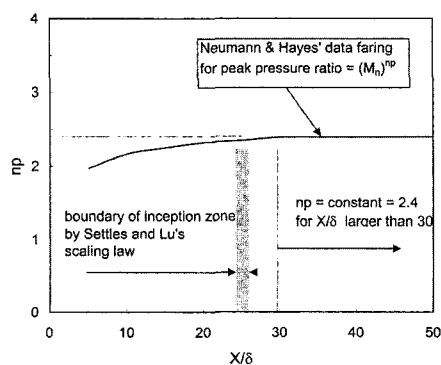


Fig. 5 Exponent in peak pressure correlation by Neumann and Hayes

for their experiments. By applying Settles and Lu's scaling law shown in Eq. (2) to the present experimental data, the inception length has been recalculated, and it is plotted in X/δ coordinate in Fig. 5. The boundary between the inception and conical zones by the scaling law is found to lie between $X/\delta=24$ and 26 , which shows a reasonable agreement with the result of the peak pressure correlation by Neumann and Hayes.

4.3 Virtual conical origin

Since the theory of the quasi-conical symmetry is based on that all surface features in conical region are bounded by rays from a common origin (VCO), the location of VCO is a fundamental basis in the theory. As noted in Fig. 3, this origin generally does not coincide with the junction of the fin leading edge and the plate, but is located slightly upstream of the junction. The virtual origin is displaced by a distance ΔVCO along the inviscid shock line on test surface, as depicted in Fig. 2.

In spite of its important implication, the information of VCO has been sparse, except the knowledge that VCO location (or ΔVCO) is surely a viscous flow phenomenon depending on M_∞ and δ , and that the ΔVCO decreases as the shock strength increases. The simplest method to locate the VCO is to utilize the surface flow visualization techniques, such as kerosene-lamp-black tracings, by identifying the feature of limiting streamlines from the tracings and intersecting those lines to a single point (see Fig. 3).

Instead utilizing the surface streakline patterns, Rodi and Dolling have located the virtual conical origin based upon their surface pressure data (Rodi and Dolling, 1995). In their method, they identified specific features in the pressure distribution at two rows (i.e., such as initial pressure rise, plateau, trough, etc) and passed a straight line through the locations of the same feature on different rows. Finally they could locate a VCO by determining the intersection of those pairs of lines.

However, their method has a limitation that it requires detailed information of the surface pressure data. Therefore, for the present study, the

simple kerosene-lampblack tracings have been utilized to estimate the location of VCO. For a couple of interaction cases, both the surface flow visualization and Rodi and Dolling's methods have been applied to locate VCO. The results have been compared each other, and it is confirmed that both results have reasonable agreements for most cases.

When the location of VCO is estimated by the surface steakline patterns, the lines through surface flow features do not collapse occasionally to a single point. There are certain errors associated with the procedure, and an optimized collapse-point of those lines should be chosen. The uncertainty of the VCO location has thus been estimated, and it is found that the uncertainty of the ΔVCO is approximately ± 2 incoming boundary layer thicknesses along the inviscid shock line for the present experiments.

Since the location of the virtual conical origin is displaced by ΔVCO from the fin leading edge along the inviscid shock line (see Fig. 2), it is possible to estimate the location of VCO from the scaling law of the upstream influence. It is done by simply extending the conical asymptote of the upstream influence line to the virtual conical origin in the nondimensionalized coordinate shown in Fig. 4. Figure 6 shows this estimation procedure. From the error band of the boundary dividing the inception and conical zones, two extreme conical asymptotes have been utilized to estimate the location of VCO. In Fig. 6, it is noticed ;

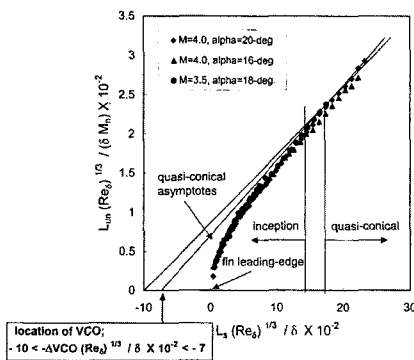


Fig. 6 Estimation of the virtual conical origin by the scaling law of upstream influence

$$7 \leq \Delta VCO(Re_{\delta}^{1/3}) / \delta \times 10^{-2} \leq 10 \quad (4)$$

and thus,

$$700 \delta / (Re_{\delta}^{1/3}) \leq \Delta VCO \leq 1000 \delta / (Re_{\delta}^{1/3}) \quad (5)$$

The simple Eq. (5) shows that the location of VCO is dependent on δ and $Re_{\delta}^{1/3}$, but it is dependent on neither freestream Mach number, M_{∞} , nor the normal Mach number, M_n . However, this result is questionable, since the VCO is surely a phenomenon of highly compressible viscous flows, and thus should be dependent on the incoming boundary layer thickness and the freestream Mach number (or, the normal Mach number) by some ways.

Figure 7 shows the present experimental results of VCO locations obtained by the surface flow visualization for various shock strengths (i.e., for various values of M_n). For the cases of the freestream Mach numbers of 2.5 and 3.5, the experimental data by Lu (Lu, 1988) have been utilized. In the figure, it is noticed that the estimation of ΔVCO by Eq. (5) does not show good agreement with the present experimental results. It is obvious that the ΔVCO is surely dependent not only on the freestream Mach number but on the shock strength (i.e., normal Mach number). It is also noticed that the ΔVCO becomes smaller as the normal Mach number increases.

However, in Fig. 7, implying that the ΔVCO is dependent on the characteristics of the incoming boundary layer and the freestream Mach number, Settles and Lu's scaling law shown in Eq. (1) is presumed to be still valid, and a slight different approach to estimate the location of ΔVCO can

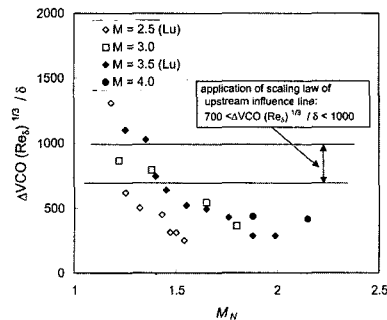


Fig. 7 Comparison of the experimental VCO locations with the result by the scaling law

be tried. After a coordinate parameter depending on M_n and $Re_\delta^{1/3}$ is made according to the scaling law, and the correlation of the normalized ΔVCO with respect to δ with the new coordinate parameter has thus been performed.

Figure 8 shows the result of the correlation. Uncertainty levels of the VCO location equal to ± 2 incoming boundary layer thicknesses for the present experiments are also depicted in the figure. In Fig. 8, it is noticed that the correlation of the normalized ΔVCO with $M_n^2/Re_\delta^{1/3}$ shows a reasonable result, and the correlation equation is;

$$\Delta VCO/\delta \approx 270(100 \times M_n^2/Re_\delta^{1/3})^{-3.5} + 5 \quad (6)$$

For the weakest interaction, such as for the freestream Mach number of 2.5, the VCO is some significant distance upstream of the fin leading edge. It is also noticed that the normalized VCO decreases as $M_n^2/Re_\delta^{1/3}$ increases. The scaling law associated with M_n and $Re_\delta^{1/3}$ is presumed to be still valid, and the strong dependency of the normalized VCO to the normal Mach number (i.e., M_n^2) is another demonstration of the quasi-conical characteristics of the fin interactions. The present correlation is thus proposed to estimate ΔVCO for a wide range of interaction strengths of M_∞ from 2.5 to 4.0.

One possible limitation in the correlation is that the range of Reynolds numbers of the experimental data utilized in the correlation are somewhat narrow. All data have been taken for high unit Reynolds number flows, typically in the range between $5 \times 10^7/m$ and $7 \times 10^7/m$. Further

detailed investigation for wider range of Reynolds number flows on the correlation of ΔVCO is thus suggested for the future study.

Conclusions

An experimental study on the quasi-conical symmetry in swept shock wave/turbulent boundary-layer interactions has been performed. When an equilibrium turbulent boundary layer on a flat plate is subjected to interact with swept planar shock waves, the interaction flowfield has a nature of conical symmetry. Surface streakline patterns obtained from the kerosene-lampblack tracings have been utilized to estimate representative surface features of the flows, such as the upstream influence and the virtual conical origin. The scaling law of the interaction suggested by previous investigators has been reexamined for different freestream Mach numbers. It is noticed that the present experimental data reasonably agrees with the scaling law of upstream influence and the previous result of the peak pressure correlation. Application of the law by simply extending the conical asymptote of the upstream influence line is not appropriate to estimate the location of the virtual conical origin. However, the scaling law associated with M_n and $Re_\delta^{1/3}$ is presumed to be still valid, if slightly modified, and finally a correlation equation of the ΔVCO has been proposed.

Acknowledgments

The author would like to gratefully acknowledge the many useful discussions with R. D. Neumann of Air Force Research Laboratory, OH, USA.

References

- Alvi, F. S. and Settles, G. S., 1991, "Physical Flowfield Model of the Swept Shock/Boundary-Layer Interaction Flowfield," AIAA Paper 91-1768.
- Dolling, D. S. and Bogdonoff, S. M., 1983, "Upstream influence in Sharp Fin-Induced

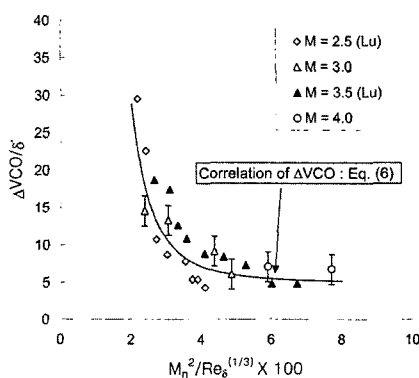


Fig. 8 A correlation of ΔVCO

Shock Wave Turbulent Boundary-Layer Interaction," *AIAA Journal*, Vol. 21, pp. 143~145.

Inger, G. R., 1987, "Spanwise Propagation of Upstream Influence in Conical Swept Shock Boundary-Layer Interactions," *AIAA Journal*, Vol. 25, pp. 287~293.

Kim, K-S., Lee, Y., Alvi, F. S., Settles, G. S. and Horstman, C. C., 1991, "Laser Skin Friction Measurements and CFD Comparison of Weak-to-Strong Swept Shock/Boundary Layer Interactions," *AIAA Journal*, Vol. 29, No. 10, pp. 1643~1650.

Lee, Y., Settles, G. S. and Horstmann, C. C., 1994, "Heat Transfer Measurements and Computations of Swept-Shock-Wave/Boundary-Layer Interactions," *AIAA Journal*, Vol. 32, No. 4, pp. 726~734.

Lu, F. K., 1988, "Fin Generated Shock-Wave Boundary-Layer Interactions," Ph. D. thesis, ME dept., The Pennsylvania State University.

Neumann, R. D. and Hayes, J. R., 1977, "Prediction Techniques for the Characteristics of the 3-D Shock Wave Turbulent Boundary-Layer Interactions, AIAA paper 77-46," *AIAA 15th Aerospace Science Meeting*.

Rodi, P. E. and Dolling, D. S., 1995, "Behavior of Pressure and Heat Transfer in Sharp Fin-Induced Turbulent Interactions," *AIAA Journal*, Vol. 33, No. 11, pp. 2013~2019.

Settles, G. S., 1975, "An Experimental Study of Compressible Turbulent Boundary Layer Separation at High Reynolds numbers," Ph. D. Thesis, Aerospace and Mechanical Sciences Department, Princeton University, N. J.

Settles, G. S. and Dolling, D. S., 1986, "Swept Shock Wave Boundary-Layer Interactions," in *AIAA Progress in Astronautics and Aeronautics: Tactical Missile Aerodynamics* (Edited by M. Hemsch and J. Nielsen), Vol. 104, pp. 297~379, AIAA, New York.

Settles, G. S. and Lu, F. K., 1985, "Conical Symmetry of Shock/Boundary-Layer Interactions Generated by Swept and Unswept Fins," *AIAA Journal*, Vol. 23, pp. 1021~1027.

Zubin, M. A. and Ostapenko, N. A., 1979, "Structure of Flow in the Separation Region Resulting from Interaction of a Normal Shock Wave with a Boundary Layer in a Corner," *Izvest. Akad. Nauk S. S. S. R., Mekh, Zhid. I Gaza*, No. 3, pp. 51~58 (English trans.)

Correction to “An Adaptive Algorithm Applied to a Design of Robust Observer [1]” The authors’ names were misplaced in the paper [1], and they are corrected as follows :

Hyungbo Shim, Young-Ik Son, Juhoon Back and Nam-Hoon Jo, 2003, “An Adaptive Algorithm Applied to a Design of Robust Observer,” KSME International Journal, Vol. 17, No. 10, pp. 1443~1449.

References

- [1] Young-Ik Son, Hyungbo Shim, Juhoon Back and Nam-Hoon Jo, 2003, “An adaptive algorithm applied to a design of robust observer,” KSME International Journal, Vol. 17, No. 10, pp. 1443~1449.